TUM/T39-03-30

Why a long-lived fireball can be compatible with HBT measurements *)

Thorsten Renk[a]

[a] *Physik Department, Technische Universität München, D-85747 Garching, GERMANY*

Abstract

The common interpretation of HBT data measured at top SPS energies leads to apparent source lifetimes of 6–8 fm/c and emission duration of approximately 2–3 fm/c. We investigate a scenario with continuous pion emission from a long-lived ($\sim$ 16 fm/c) thermalized source in order to show that it is not excluded by the data. Starting from a description of the source's spacetime expansion based on gross thermodynamical properties of hot matter (which is able to describe a number of experimental observables), we introduce the pion emission function with a contribution from continuous emission during the source's lifetime and another contribution from the final breakup and proceed by calculating the HBT parameters R_{out} and R_{side}. The results are compared with experimental data measured at SPS for 158 AGeV central Pb-Pb collisions. We achieve agreement with data, provided that some minor modifications of the fireball evolution scenario are made and find that the parameter R_{out} is not sensitive to the fireball lifetime, but only to the duration of the final breakup, in spite of the fact that emission takes place throughout the whole lifetime. We explicitly demonstrate that those findings do not alter previous results obtained within this framework.

1 Introduction

One of the main goals in the study of ultrarelativistic heavy-ion collisions (URHIC) is to understand the conditions realized in the center of such a collision. If the created system is sufficiently thermalized, one can in principle link measurements with information coming from lattice simulations about the equation of state (EoS) of hot QCD matter (see e.g. [1]). However, in order to make use of the EoS, some information on the spatial expansion pattern of the matter is extremely helpful.

HBT correlation measurements can provide at least part of this information (see [2, 3] for a review). However, such measurements can only reveal the correlation lengths of the source, which result from a complex interplay of temperature, flow pattern and true geometrical shape. Commonly, simple (often Gaussian) parameterizations of the emission source are used to interpret the experimental information and extract the geometrical (Gaussian) radius of the source R_G, its transverse expansion velocity $v_\perp$, from the longitudinal correlation radius R_{long} the source lifetime τ_f and from R_{out}/R_{side} its emission duration $\Delta\tau$. In [4] (discussing HBT measurements of Pb-Pb collisions at SPS), these parameters are found to be $R_G \approx 6$ fm, $\tau_f \approx 6-8$ fm/c, $v_\perp \approx 0.5c$ and $\Delta\tau \approx 2-3$ fm/c for an assumed temperature at breakup of $T_f = 120$ MeV. These numbers point to a rather rapidly expanding and decaying system.

However, there is a subtle problem with this interpretation: If the system expands from a root mean sqare radius R_{rms} of about 4.5 fm (as found by a calculation of the overlap of the colliding nuclei) to the measured R_{rms} of about 8.5 fm (assuming $R_G = 6$ fm), while at the same time the fireball front (for a Gaussian distribution, take e.g. R_{rms} for the front) expands to a velocity of $\sim 0.5c$, we may expect the following equations to approximate the problem [10]:

$$R_{rms}(\tau_f) - R_{rms}(0) = \frac{a}{2}\tau_f^2 \qquad \text{and} \qquad v_\perp(\tau_f) = a \cdot \tau_f \tag{1}$$

*)work supported in part by BMBF and GSI

Solving for a and τ_f we find $\tau_f \approx 15$ fm/c, clearly incompatible with the lifetime extracted from R_{long}. What is wrong here?

In [10], it has been pointed out that the relation [5]

$$R_{long} = \tau_f (T_f/m_t)^{1/2} \tag{2}$$

(with transverse mass $m_t = \sqrt{p_t^2 + m^2}$ and p_t the transverse momentum of a particle with mass m) linking the measured R_{long} and τ_f is based on a backwards extrapolation of the measured freeze-out state, assuming that the longitudinal expansion takes place with the same velocity at all times before τ_f. However, this relation ceases to hold if the system undergoes accelerated longitudinal expansion also (in this case, the lifetime can be significantly longer than extracted from (2)), so the estimate done from the transverse dynamics is probably more reliable.

This, however, immediately gives rise to the following question: If a thermal source expands for $O(15)$ fm/c, how can it be that its apparent emission duration is only $O(2)$ fm/c? In order to answer this question, one needs to specify the space-time evolution of the source beyond the schematic parameterization used in [4]. We will employ a description of this evolution based on bulk thermodynamic properties of the fireball to investigate this question.

The paper is organized as follows: After an introduction to the fireball expansion model, we discuss in greater detail why longitudinal acceleration helps to match the timescales extracted from R_{long} and R_{side}. Then we specify how this model is used to calculate the relevant HBT parameters. We subsequently compare the results to the measured data and explicitly demonstrate the differences to the standard parameterizations. Then we discuss the modifications to our scenario which are required to obtain good agreement with the data. Finally we investigate the physics behind the observed long fireball lifetime and the small difference between R_{out} and R_{side} and discuss the impact of the modifications introduced before to previous results obtained within the same framework.

2 Fireball evolution and hadron emission

In this section, we briefly outline the general framework of the fireball evolution model which we use in the following as a starting point for the calculation of hadron emission and ultimately the calculation of HBT radius parameters.

2.1 Expansion and flow

Our fundamental assumption is to treat the fireball matter as thermalized from an initial proper time scale τ_0 until breakup time τ_f. For simplicity, we assume a spatially homogeneous distribution of matter. Since some volume elements move with relativistic velocities, it is sensible to choose volumes corresponding to a given proper time τ for the calculation of thermodynamics, hence the thermodynamic parameters temperature T, entropy density s, pressure p, chemical potentials μ_i and energy density ϵ become functions of τ only for such a system. In the following, we refer to τ as the time measured in a frame co-moving with a given volume element.

In order to make use of the information coming from lattice QCD calculations, we proceed by calculating the thermodynamical response to a volume expansion that is parametrized in such a way as to reproduce the experimental information about the flow pattern and HBT correlations as closely as possible.

As a further simplification, we assume the volume to be cylindrically symmetric around the beam (z)-axis. Thus, the volume is characterized by the longitudinal extension $L(\tau)$ and the transverse radius

$R(\tau)$ and we find

$$V(\tau) = \pi L(\tau) R^2(\tau). \tag{3}$$

In order to account for collective flow effects, we boost individual volume elements according to a position-dependent velocity field. For the transverse flow, we make the ansatz

$$\eta_T(r,\tau) = r/R_{rms}(\tau)\eta_T^{rms}(\tau) \tag{4}$$

where $R_{rms}(\tau)$ denotes the root mean square radius of the fireball at τ and $\eta_T^{rms}(\tau)$ the transverse rapidity at R_{rms}.

For the longitudinal dynamics, we start with the experimentally measured width of the rapidity interval of observed hadrons $2\eta_f^{front}$ at breakup. From this, we compute the longitudinal velocity of the fireball front at kinetic freeze-out v_f^{front}. We do not require the initial expansion velocity v_0^{front} to coincide with v_f^{front} but instead allow for a longitudinally accelerated expansion. This implies that during the evolution $\eta = \eta_s$ is not valid (with $\eta = \text{atanh}\ v$ and η_s the spacetime rapidity $\eta_s = 1/2 \ln(t+z)/(t-z)$) in contrast to the non-accelerated case.

The requirement that the acceleration should be a function of τ and that the system stays spatially homogeneous for all τ determines the velocity field uniquely once the motion of the front is specified. We solve the resulting equations numerically [6] and find that for not too large rapidities $\eta < 4$ and accelerations volume elements approximately fall on curves $const. = \sqrt{t^2 - z^2}$ and that the flow pattern can be approximated by a linear relationship between rapidity η and spacetime rapidity η_s as $\eta(\eta_s) = \zeta\eta_s$ where $\zeta = \eta^{front}/\eta_s^{front}$ and η^{front} is the rapidity of the cylinder front. In this case, the longitudinal extension can be found calculating the invariant volume $V = \int d\sigma_\mu u^\mu$ as

$$L(\tau) \approx 2\tau \frac{\sinh\left((\zeta-1)\eta_s^{front}(\tau)\right)}{(\zeta-1)} \tag{5}$$

with $\eta_s^{front}(\tau)$ the spacetime rapidity of the cylinder front. This is an approximate generalization of the boost-invariant relation $L(\tau) = 2\eta^{front}\tau$ which can be derived for non-accelerated motion. A more detailed description of the expansion can be found in [6].

2.2 Parameters of the expansion

In order to proceed, we have to specify the longitudinal acceleration $a_z(\tau)$ at the fireball front (which in turn is used to calculate $\eta_s^{front}(\tau)$ numerically), the initial front velocity v_0^{front} and the expansion of the radius $R(\tau)$ in proper time.

We make the ansatz

$$a_z = c_z \cdot \frac{p(\tau)}{\epsilon(\tau)} \tag{6}$$

which allows a soft point in the EoS where the ratio p/ϵ gets small to influence the acceleration pattern. c_z and v_0^{front} are model parameters governing the longitudinal expansion and fit to data.

Since typically longitudinal expansion is characterized by larger velocities than transverse expansion, i.e. $v_z^{front} \gg v_T^{front}$, we treat the radial expansion non-relativistically. We assume that the radius of the cylinder can be written as

$$R(\tau) = R_0 + c_T \int_{\tau_0}^{\tau} d\tau' \int_{\tau_0}^{\tau'} d\tau'' \frac{p(\tau'')}{\epsilon(\tau'')} \tag{7}$$

The initial radius R_0 is taken from overlap calculations. This leaves a parameter c_T determining the strength of transverse acceleration which is also fit to data. The final parameter characterizing the expansion is its endpoint given by τ_f, the breakup proper time of the system.

2.3 Thermodynamics

We assume that entropy is conserved throughout the thermalized expansion phase. Therefore, we start by fixing the entropy per baryon from the number of produced particles per unit rapidity (see e.g. [7]). Calculating the number of participant baryons (see [8]) we find the total entropy S_0. The entropy density at a given proper time is then determined by $s = S_0/V(\tau)$.

We describe the EoS in the partonic phase by a quasiparticle interpretation of lattice data which has been shown to reproduce lattice results both at vanishing baryochemical potential μ_B and finite μ_B [11] (see these references for details of the model).

In the hadron gas phase, we calculate thermodynamic properties at kinetic decoupling where interactions cease to be important. Here, we have reason to expect that an ideal gas will be a good description. Determining the EoS at this point, we choose a smooth interpolation from here to the EoS obtained in the quasiparticle description. This is described in greater detail in [8, 9].

With the help of the EoS and $s(\tau)$, we are now in a position to compute the parameters $p(\tau), \epsilon(\tau), T(\tau)$ as well. Since the ratio $p(\tau)/\epsilon(\tau)$ appear in the expansion parametrization, we have to solve the model self-consistently.

2.4 Solving the model

In order to adjust the model parameters, we compare with data on transverse momentum spectra and HBT correlation measurements. In [10], a similar model is fit to a large set of experimental data, providing sets of parameters $T_f, v_{\perp f}, R_f, \eta_f^{front}$ at freeze-out. Although the present model uses a different (box vs. Gaussian) longitudinal distribution of matter, we use the parameters from this analysis as a guideline for the transverse dynamics where this difference should not show up and determine η_f^{front} separately. Specifically, we use the set **b1** from [10] for the transverse dynamics.

By requiring $R(\tau_f) = R_f$ and $v_T^{front} = v_{\perp f}$ we can determine the model parameters c_T and τ_f. c_z is fixed by the requirement $\eta^{front}(\tau_f) = \eta_f^{front}$. The remaining parameter v_0^{front} now determines the volume (and hence temperature) at freeze-out and can be adjusted such that $T(\tau_f) = T_f$.

The model for 5% central 158 AGeV Pb-Pb collisions at SPS is characterized by the following scales: Initial long. expansion velocity $v_0^{front} = 0.5c$, thermalization time $\tau_0 = 1$ fm/c, initial temperature $T_0 = 305$ MeV, duration of the QGP phase $\tau_{QGP} = 7$ fm/c, duration of the hadronic phase $\tau_{had} = 9$ fm/c, total lifetime $\tau_f - \tau_0 = 16$ fm/c, r.m.s radius at freeze-out $R_f^{rms} = 8.55$ fm, transverse expansion velocity $v_{\perp f} = 0.537c$.

2.5 Initial compression and re-expansion

We have chosen the above model framework in such a way that it allows to account for the apparent mismatch in timescales derived from Eqs. (1) and (2). This is done by allowing for initial compression of the matter in longitudinal direction and subsequent re-expansion. The longitudinal flow pattern of matter is schematically indicated in Fig. 1.

It is apparent from the figure that a measurement of the conditions around the freeze-out hypersurface $\tau = \tau_f$ (where the bulk of hadronic emission takes place) would not be able to distinguish between an accelerated or non-accelerated longitudinal evolution history. This has also been pointed out in [10]. Hence, incorporating accelerated longitudinal expansion we have the freedom to select τ_f accoring to Eq. (1) without being in contradiction with (2). (Since we in practice adjust the model to R_{long} and the observed multiplicity distribution in rapidity, a detailed discussion of R_{long} in this paper is not fruitful).

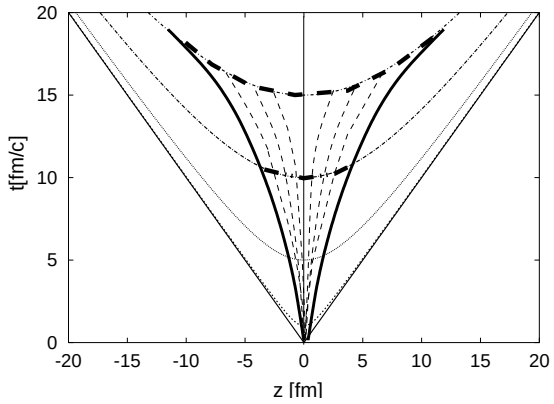

Figure 1: A scetch of the accelerated longitudinal expansion pattern of the fireball matter.

In our model, the parameter controlling the initial amount of compression is $v_0^{front} = 0.5c$. This has profound consequences for the initial state: If we set $v_0^{front} = v_f^{front}$ (and hence use the scenario underlying Eq. (2)), the initial temperature of the fireball drops by $\sim 30\%$.

This in turn has consequences for the emission of real photons. In [12] it was shown that a scenario very similar to the one discussed here can account for the measured amount of photon emission, especially in the momentum region between 2 and 2.5 GeV where no significant prompt photon contribution is expected. Assuming a scenario without longitudinal acceleration, the yield of direct photons at 2 GeV drops by a factor 8 for the standard choice of the equilibration time of $\tau_0 \approx 1$ fm/c in striking disagreement with tha data. This cannot fully be compensated even for a choice of the equilibration time as low as 0.1 fm/c.

In conclusion, the longitudinally accelerated pattern advocated earlier to explain the difference between the timescales extracted from (1) and (2) is strongly favoured by the direct photon data. Therefore, we will assume in the following that the relevant timescale of the fireball evolution can be inferred from transverse dynamics only and focus on the remaining question of the apparent mismatch of the source evolution time $O(15)$ fm/c and its emission duration $O(2)$ fm/c. In order to investigate this, we have to specify the emission function of the fireball.

2.6 Hadron emission from the hypersurface with timelike normal

One contribution to the total emission of particles from the fireball comes from the final breakup of the thermalized system. The corresponding freeze-out hypersurface is characterized by a timelike normal. We calculate particle emission from this phase with the help of the emission function

$$\begin{aligned} S_t^i(x,K)d^4x = & \frac{M_T \cosh(Y-\eta_s)}{(2\pi)^3} \exp\left(\frac{K\cdot u(x)+\mu_i}{T_f} \pm 1\right)^{-1} \cdot G(r)H(\eta_s)d\eta_s r dr d\phi \\ & \times \frac{\tau d\tau}{\sqrt{2\pi(\Delta\tau)^2}} \exp\left(-\frac{(\tau-\tau_f)^2}{2(\Delta\tau)^2}\right) \end{aligned} \tag{8}$$

In this expression, the momentum K is parametrized in terms of longitudinal rapidity Y, transverse mass $M_T = \sqrt{K_t^2 + m_i^2}$ and transverse momentum K_t The factor $\exp\left(\frac{k\cdot u(x)+\mu_i}{T_f} \pm 1\right)^{-1}$ corresponds to

the thermal distribution of particle species i (with corresponding chemical potential μ_i and mass m_i) where the product $k \cdot u(x)$ takes care of evaluating the distribution in the rest frame of matter moving with four-velocity $u(x)$ as seen from a particle with momentum K and the $+(-)$ sign holds for fermions (bosons). $G(r)$ and $H(\eta_s)$ describe the distribution of matter in radial and longitudinal direction using the radius r and spacetime rapidity η_s. Finally, the factor $\exp\left(-(\tau-\tau_f)^2/(2(\Delta\tau)^2)\right)$ can be seen as a smearing of a sudden decoupling occuring at proper time τ_f into an extended breakup time period characterized by $\Delta\tau$.

The single particle spectrum for particle species i is calculated from this emission function as

$$E_p^i \frac{dN_i}{d^3p} = \int d^4x S_t^i(x,p) \tag{9}$$

with $E_p^i = \sqrt{p^2+m_i^2}$. HBT correlation radii are obtained using the common Cartesian parametrization

$$C(q,K) - 1 = \exp\left[-q_o^2 R_{out}^2(K) - q_s^2 R_{side}^2(K) - q_l^2 R_{long}^2(K) - 2q_o q_l R_{ol}^2(K)\right] \tag{10}$$

(see e.g. [2, 3] for an overview and further references) for the correlator. Here, $K = \frac{1}{2}(p_1+p_2)$ is the averaged momentum of the correlated pair with individual momenta p_1, p_2 and $q = (p_1 - p_2)$ the momentum difference. The transverse correlation radii $R_{out,side}$ follow from the emission function as

$$R_{side}^2 = \langle \tilde{y}^2 \rangle \tag{11}$$

$$R_{out}^2 = \langle (\tilde{x} - \beta_\perp \tilde{t})^2 \rangle \tag{12}$$

with $\beta_\perp$ the transverse velocity of the emitted pair, $\tilde{x}_\mu = x_\mu - \langle x_\mu \rangle$ and

$$\langle f(x) \rangle (K) = \frac{\int d^4x f(x) S(x,K)}{\int d^4x S(x,K)} \tag{13}$$

an average with the emission function.

In [10], expressions (9), (11) and (12) have been used to fit the parameters of the shapes $G(r)$ and $H(\eta)$, the radial and longitudinal expansion velocities at freeze-out τ_f, the freeze-out temperature T_f and the temporal smearing $\Delta\tau$ to experiment, thus providing the basic parameters for the fireball evolution described above. As a starting point for the investigations in this paper, we assume a box profile $G(r) = \theta(R_B - r)$ for the radial distribution of thermalized matter. We use $H(\eta_s) = \theta(\eta_s^{front}(\tau_f) - \eta_s)\theta(\eta_s^{front}(\tau_f) + \eta_s)$ throughout this paper.

2.7 Hadron emission from the hypersurface with spacelike normal

In addition to particle emission at the final breakup of the fireball described by (8), there is also continuous emission of particles throughout the whole lifetime of the system. Such emission is characterized by a freeze-out hypersurface with spacelike normal.

Since the correlation radius R_{out} probes not only the geometrical radius of the source, but also the duration of particle emission (see Eq. (12)), it may well be that such a contribution significantly change the ratio R_{out}/R_{side} (which is known to be small experimentally) as compared to the use of only the emission function (8).

In order to investigate this question, we consider in addition to (8) also the emission function

$$S_s^i(x,K)d^4x = \frac{1}{(2\pi)^3}\left(K_\perp\cos(\phi) - v_\perp(\tau)M_T\cosh(Y-\eta_s)\right)\cdot\theta\left(K_\perp\cos(\phi) - v_\perp(\tau)M_T\cosh(Y-\eta_s)\right)$$
$$\times\exp\left(\frac{K\cdot u(x)+\mu_i^B}{T_B}\pm 1\right)^{-1} d\eta_s r dr d\phi\tau d\tau\delta(r-R_B(\tau))\theta(\eta_s+\eta_s^{front}(\tau))$$
$$\times\theta(\eta_s^{front}(\tau)-\eta_s)\theta(\tau-\tau_i)\theta(\tau_f-\tau) \tag{14}$$

which describes the emission of particles with transverse velocity $K_\perp/E_K\cos(\phi)$ from the fireball surface moving at $v_\perp$ (with ϕ the angle between surface and the momentum vector of the emitted particle) at $r = R_B(\tau)$ between the space-time rapidity extent of the fireball from $+\eta_f(\tau)$ to $-\eta_f(\tau)$ between initial time τ_i and freeze-out time τ_f. The factor $\theta\left(\frac{K_\perp}{E_K}\cos(\phi) - v_\perp(\tau)\right)$ ensures that emission only takes place for particles moving faster than the emission surface and no negative contribution of 'backward emission' are counted.

We assume that the expanding fireball can be described as a hot 'core' and a (thin) boundary region from which the emission takes place. This region is assumed to be characterized by an average temperature T_B. We do not require $T_B = T_f$, but leave this as a free parameter, however we do require that the boundary is characterized by the same pion density as the whole fireball at breakup, which fixes μ_i^B for given T_B.

To a first approximation, we describe the total particle emission by the sum of both emission throughout lifetime and final breakup as $S^i(x,k) = S_t^i(x,k) + S_s^i(x,k)$.

3 Calculation of HBT correlation parameters

3.1 R_{side} and the freeze-out geometry

The experimental results for the correlation radius R_{side} are often fit by a function of the form

$$R_{side} = \frac{R_G}{\sqrt{1+m_t\eta_{\perp f}^2/T_f}}. \tag{15}$$

This expression comes from an approach where only the final breakup of the fireball is taken into account, the matter distribution $G(r)$ is assumed to be Gaussian with width R_G, and Boltzmann statistics instead of Bose-Einstein statistics is used.

In contrast, in this paper we study a model with a long duration of the emission (throghout the complete fireball lifetime of ~ 17 fm/c), and a final breakup, which is characterized rather by a box-shaped transverse distribution . In addition, we use the Bose-Einstein (Fermi-Dirac) distribution where appropriate.

Evidently, the analytic expression (15) is only able to determine the ratio $\eta_{\perp f}^2/T$. Assuming $T_f = 120$ MeV, the fit yields $R_G \approx 7$ fm corresponding to $R_{rms} \approx 9.8$ fm and $\overline{v}_\perp = 0.55c$ for the most central collisions at 158 AGeV [4]. (Compare with the parameters in our fireball evolution scenario $T_f = 100$ MeV, $\overline{v}_\perp = 0.537c$ and $R_{rms} = 8.55$ fm.)

For the sake of clarity, we start by presenting the result of evaluating (11) using $S_t^\pi(x,K)$ only, i.e. we neglect all emission throughout the fireball lifetime. The result is shown in Fig. 2.

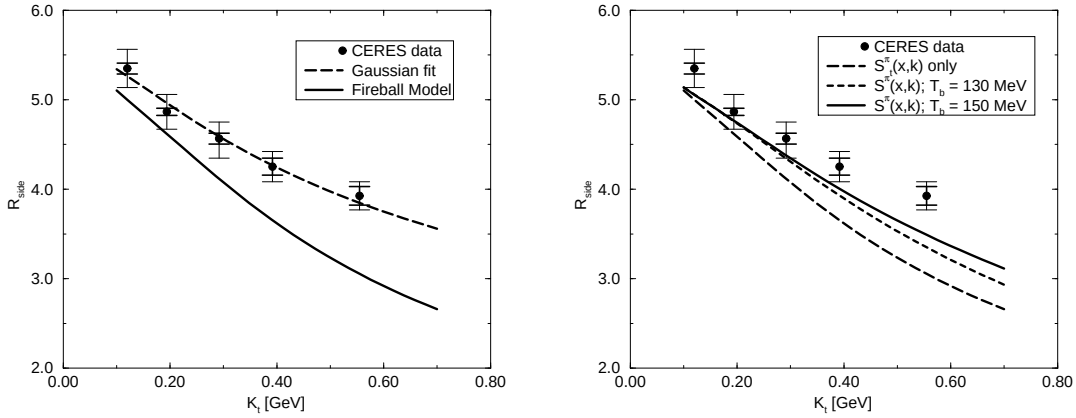

Figure 2: Left panel: CERES data on R_{side} for central Pb-Pb collisions at 158 AGeV with statistical (small bars) and systematical (large bars) errors (unmerged), in addition to a fit to data based on a Gaussian source and the result based on the box profile used in our fireball evolution scenario, considering breakup at τ_f only. Right panel: Data as before, shown is emission only at fireball breakup (dashed), and the results with the full emission function for two different values of the average temperature of the emission layer (dotted and solid).

Clearly, the overall normalization (set by the R_{rms} radius) appears too small in the model and the falloff with transverse pair momentum K_t too steep.

The latter effect can be explained by the observation that the Gaussian distribution allows for a (small) component of the total amount of matter to be at large radii and hence to be boosted with large radial velocities if a flow profile as in Eq. (4) is chosen, whereas the box profile used in the present scenario does not.

This discrepancy is significantly reduced by using the full emission function $S^\pi(x,K)$ instead of $S^\pi_t(x,K)$. This is due to the fact that emission of fast particles is preferred for a freeze-out hypersurface with spacelike normal, leading to an enhancement of the correlation radii at larger K_t also (Fig. 2, right panel). In addition, we have some freedom to adjust T_B (the average temperature of the emitting region in $S^\pi_s(x,K)$) within reasonable limits. The data prefer a rather large value $T_B \sim 150$ MeV. This should not come as a surprise, since the temperature of the emitting layer may well be large in the initial stages of fireball evolution.

Guided by the success of the Gaussian parametrization, we drop the unphysically sharp cutoff of the box profile $G(r) = \theta(R_{box} - r)$ and use instead a Woods-Saxon distribution (retaining the value of $T_B = 150$ MeV in the following)

$$G(r) = \frac{1}{1 + \exp\left[\frac{r - R_{box}}{d_{WS}}\right]} \tag{16}$$

We find that the data prefer rather small values of d_{WS} of the order of 0.8 fm (see Fig. 3, left panel). This is reassuring since it gives some justification for the use of a box profile in the calculation of dilepton and photon emission.

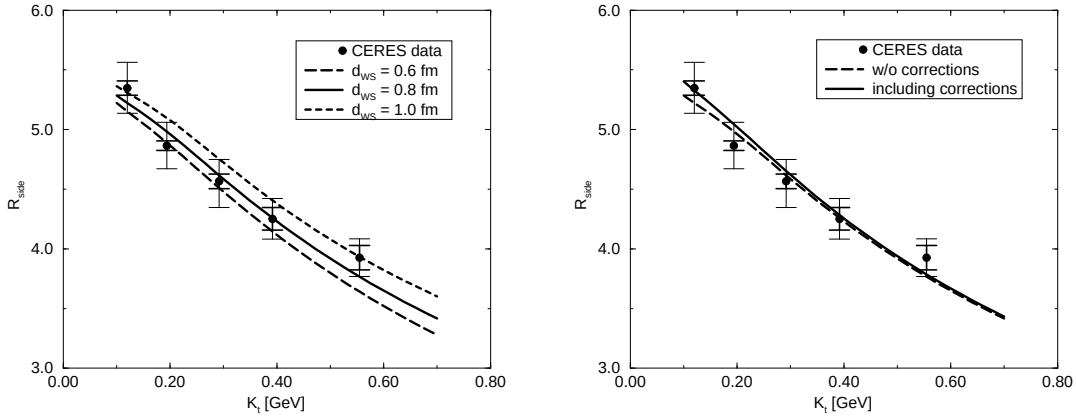

Figure 3: Left panel: CERES data on R_{side} for central Pb-Pb collisions at 158 AGeV with statistical (small bars) and systematical (large bars) errors (unmerged). Left panel: Calaulated R_{side} for various values of the Woods-Saxon skin thickness parameter d_{WS}. Right panel: Calculated R_{side} using $d_{WS} =$ 0.8 fm (dashed), shown is the effect of model-independent correction terms (17) (solid).

Finally, we also calculate the model-independent corrections [15] to (11)

$$\Delta R^2_{side} = \left(\frac{1}{4K_\perp} \frac{d}{dK_\perp} - \frac{1}{2} \frac{d}{dm^2} \right) \ln \int d^4x S^\pi(x,K), \tag{17}$$

which primarily affect the low momentum region. This is shown in Fig. 3, right panel. These corrections are small, however, they tend to improve agreement with data slightly in the low K_t region.

In summary, including the emission throughout the fireball lifetime and all correction terms, we achieve a good description of the experimental data.

3.2 R_{out} and the freeze-out criterion

It is commonly deduced from (11) and (12) that the duration of pion emission can be calculated as

$$\Delta\tau^2 = \frac{1}{\beta_t^2}(R^2_{out} - R^2_{side}) \tag{18}$$

with β_t the velocity of the emitted pair $\beta_t = K_t/E_K$. However, there are in fact two different timescales related to the duration of the emission in our model: a) the total lifetime of the fireball of order ~ 17 fm/c and b) the duration of the final breakup, which is a priori unknown, but can be expected to be of order of at most a few fm/c for the whole evolution scenario to make sense. We therefore expect the actual difference between R_{out} and R_{side} in our model to be characterized by a mixture of these two scales, weighted with their respective contribution to the total pion emission.

We start the investigation of R_{out} by fixing all parameters at the value used to describe R_{side} and evaluating (12) with different values of $\Delta\tau$, the final breakup duration. In all following calculations, we also include the correction term for R_{out} [15]

$$\Delta R^2_{out} = \left(\frac{1}{4} \frac{d^2}{dK_t^2} - \frac{1}{2}(1-\beta_\perp^2) \frac{d}{dm^2} \right) \ln \int d^4x S^\pi(x,K) \tag{19}$$

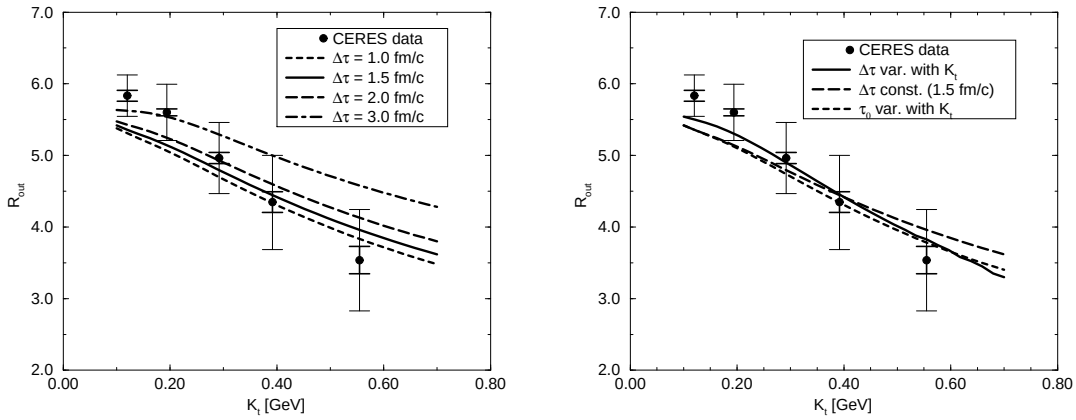

Figure 4: CERES data on R_{out} for central Pb-Pb collisions at 158 AGeV with statistical (small bars) and systematical (large bars) errors (unmerged). Left panel: Calculated R_{out} for different values of the fireball breakup time $\Delta\tau$. Right panel: R_{out} for different momentum-dependent freeze-out scenarios (see main text)

The result is shown in Fig. 4.

Clearly, the overall magnitude of the calculated R_{out} is in agreement with data, provided that a rather sudden breakup time of the order of 1–3 fm/c is choosen. This indicates that that the difference $1/\beta_t^2(R_{out}^2 - R_{side}^2)$ does not reflect the full fireball lifetime τ_f^2 but rather is dominantly influenced by $\Delta\tau$ only (otherwise one would expect the difference to be significantly larger). We will argue later on that this is so because the numerical contribtion from continuous emission throughout the fireball lifetime is small compared to the contribution from final breakup.

The shape of the falloff with K_t, however, is not well reproduced for any choice of $\Delta\tau$. (In fact, the shape appears similar to the falloff of R_{side} and rather insensitive to variations of $\Delta\tau$.) This suggests that the data (albeit the systematic errors are rather large) indicate the need for a more refined freeze-out scenario.

In [16], such a more detailed scenario based on the (momentum-dependent) mean free path of pions inside the hot matter is described. It is beyond the scope of the present paper to show that this freeze-out criterion is able to describe the data, however, we will argue that it leads to the correct qualitative behaviour of the calculated R_{out}.

The essential observation made in [16] ist that the freeze-out is different for high momentum pions than for low momentum pions: High momentum pions are expected to escape earlier.

If we want to incorporate this into our calculation, we have to make either $\Delta\tau$ or τ_f (or both) dependent on K_t, the idea being that the final breakup of the fireball occurs earlier for high momentum pions and happens faster.

In the right panel of Fig. 4, we demonstrate that the dependence of $\Delta\tau$ is able to qualitatively improve the agreement with data. To obtain an estimate for the qualitative behaviour, we assume $\Delta\tau = 2.0$ fm/c for $K_T = 100$ MeV and $\Delta\tau = 1.0$ fm/c for $K_t = 700$ MeV and interpolate linearly inbetween. In view of the large systematic uncertainties, however, we do not push this idea further by trying to aim at a perfect description of the data.

As for the dependence of τ_f on K_t, we observe that earlier freeze-out leads in general to smaller R_{out} at

larger K_t, since one probes a radially less expanded system. A suitable variation of $\Delta\tau$ might then be able to lead to a good description of the data. Again, in view of the large uncertainties we refrain from a further examination of this scenario.

4 Pion emission and fireball thermodynamics

The main result of the previous section is that R_{out} does not seem to reflect the order of magnitude of the fireball lifetime τ_f, even if continuous emission of pions is taken into account. This is a rather surprising result, and in this section we will investigate the relevant emission function $S_s^\pi(x,k)$ further in order to answer the following questions:

- Why is $\Delta\tau$ and not τ_f the dominant timescale in R_{out}?
- Does the continuous loss of pions (and nucleons) have any effect on the thermodynamics of the fireball (and hence invalidate the findings of e.g. [8])?

In order to answer these questions, we investigate the transverse velocity distributions in the c.m. frame of pions and nucleons emitted before τ_f (which can be easily calculated by integrating (14) over the fireball lifetime). The reason for choosing this particular distribution is the following: We may well imagine a process where a particle is emitted in the initial stage of the expansion. Such particle can be emitted with relatively small velocity (as seen in the c.m. frame), since the fireball initially does not expand in radial direction. If the emission velocity of such a particle is, however, smaller than the radial velocity of the fireball at τ_f, there is a chance that this already emitted particle re-enters the thermalized region. The condition reads:

$$R_B(t_E) + v_E^\perp t = R_B(t_E + t); t_E + t < t_f \tag{20}$$

with emission time t_E and emission velocity v_E measured in the c.m. frame. This condition is most easily implemented using the transverse velocity distribution of emitted particles.

The resulting transverse velocity distributions are shown in Fig. 5.

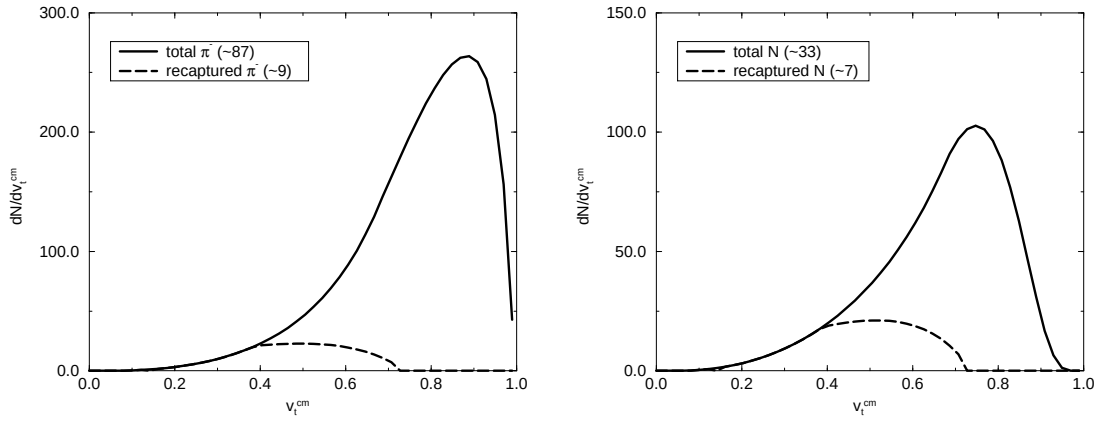

Figure 5: Left panel: Transverse velocity distribution of total π^- emission and of recaptured π^-. Right panel: Same for nucleons. Also given is the integral over the distribution.

Several important observations can be made: For the emission of pions, the recapturing process is not very efficient. This is due to the fact that the mass of the pions is of order of the temperature of

the emitting layer, hence the transverse velocity distribution is peaked towards large velocities where recapture cannot take place. On the other hand, the total number of pions emitted before the final breakup of the fireball is small as compared to the total number of observed h^- (~ 700). This explains partially the observed insensitivity of R_{out} to the fireball lifetime.

Turning to nucleons, we observe that the recapturing process is somewhat more efficient due to the large nucleon mass leading to reduced emission velocities. The total number of emitted nucleons, however, is also small as compared to the total number of participants (~ 350).

Note in addition that most of the emission takes place close to τ_f anyway, since the area of the emitting surface grows strongly with time as the fireball expands and the total number of emitted particles per unit time is proportional to this area. This is enhanced by the fact that the fireball in this scenario undergoes accelerated expansion in both in longitudinal and transverse direction, thus the emitting surface is for the larger part of the evolution significantly smaller than its final value.

We can incorporate the early loss of pions schematically into the calculation of dilepton emission (see [8])(the observable which is presumably most affected by this effect) by lowering the value of the pion chemical potential μ_π during the hadronic evolution stage (in [8], we assumed a linear rise with proper time of μ_π from 0 at the phase transition to a value consistent with the observed number of pions at thermal freeze-out. Now, we choose the endpoint such that the number of pions from both continuous emission and final breakup agrees with the observed number. We find $\mu_\pi(\tau_f) \approx 110$ MeV).

The calculation reveals that the dilepton yield in the low invariant mass region between 300 and 700 MeV is reduced by $\sim 10\%$ by the correction (this is hardly visible in a logatithmic plot, therefore we do not show a graph). Above 1 GeV invariant mass, the dilepton yield is dominated by Drell-Yan pairs and emission from the hot QGP, consequently this domain remains almost unaltered be the correction.

In summary, we conclude that it is sufficient for the description of gross thermodynamical properties of the expanding matter to approximate the fireball as a closed system which does not emit strongly interacting partcles before τ_f.

5 Conclusions

We have investigated the effect of particle emission prior to the fireball breakup time τ_f in a framework based on gross thermodynamic properties of hot QCD matter, which is nevertheless able to account for a large number of experimental observables and discussed the connection to the HBT parameters R_{out} and R_{side}.

Calculating the emission of pions from the fireball boundary and breakup, we computed R_{out} and R_{side} and compared to measurements by the CERES collaboration. We found that R_{side} can be well decribed within the present framework.

Regarding R_{out}, we identified two timescales which potentially enter this quantity, the fireball breakup time $\Delta\tau$ and the total lifetime τ_f. However, in the present framework, only $\Delta\tau$ was shown to significantly influence R_{out}. In addition, we found that a momentum-independent freeze-out criterion does not provide the best description of the data. We argued qualitatively that a more refined criterion (e.g. as suggested in [16]) improves the agreement with data.

Finally, we demonstrated that the scenario discussed here does not invalidate our previous results where we did not include the effects of continuous emission of particles from the thermalized matter.

Acknowledgements

I would like to thank W. Weise, H. Appelshäuser and A. Polleri, for interesting discussions, helpful comments and support.

References

[1] F. Karsch, E. Laermann and A. Peikert, Phys. Lett. **B 478** (2000) 447.

[2] U. A. Wiedemann and U. W. Heinz, Phys. Rept. **319** (1999) 145.

[3] B. Tomasik and U. A. Wiedemann, hep-ph/0210250.

[4] D. Adamova *et al.* (CERES collaboration), Nucl. Phys. A **714** (2003) 124; H. Tilsner and H. Appelshauser (CERES Collaboration), Nucl. Phys. A **715** (2003) 607.

[5] Y. M. Sinyukov, Nucl. Phys. **A 498** (1989) 151c.

[6] T.Renk, in preparation.

[7] J. Letessier, A. Tounsi, U. Heinz, J. Sollfrank and J. Rafelski, Phys. Rev. **D51** (1995) 3408.

[8] T. Renk, R. A. Schneider and W. Weise, Phys. Rev. C **66** (2002) 014902.

[9] T. Renk, PhD Thesis.

[10] B. Tomasik, U. A. Wiedemann and U. W. Heinz, Heavy Ion Phys. **17** (2003) 105.

[11] R. A. Schneider and W. Weise, Phys. Rev. C **64** (2001) 055201; M. A. Thaler, R. A. Schneider and W. Weise, hep-ph/0310251.

[12] T. Renk, Phys. Rev. C **67** (2003) 064901.

[13] T. Renk, Phys. Rev. C **68** (2003) 064901.

[14] A. Polleri, T. Renk, R. Schneider and W. Weise, nucl-th/0306025.

[15] S. Chapman, P. Scotto and U. W. Heinz, Heavy Ion Phys. **1** (1995) 1.

[16] B. Tomasik and U. A. Wiedemann, Nucl. Phys. A **715** (2003) 645.